The Impact of Carbonation on Hydroxide Diffusion in Nano-Confined Anion Exchange Membranes

Supporting Information

Tamar Zelovich[(1)], Cataldo Simari[(2)], Isabella Nicotera[(2),(3)],

Dario R. Dekel[(4),(5)], and Mark E. Tuckerman[(1),(6),(7)*]

1)   Department of Chemistry, New York University, New York, NY 10003, USA

2)   Department of Chemistry and Chemical Technologies, University of Calabria, Via P Bucci, 87036 Rende CS, Italy

3)   CNR-ITAE "Nicola Giordano", Via Salita S. Lucia sopra Contesse 5, Messina, 98126, Italy

4)   Wolfson Department of Chemical Engineering, Technion – Israel Institute of Technology, Haifa, 3200003, Israel

5)   Nancy & Stephen Grand Technion Energy Program, Technion – Israel Institute of Technology, Haifa, 3200003, Israel

6)   Courant Institute of Mathematical Sciences, New York University, New York, NY 10012, USA

7)   NYU-ECNU Center for Computational Chemistry, NYU Shanghai, 3663 Zhongshan Rd N, Shanghai 200062, China

Computational Methods

Each AEM system is constructed using a set of geometric requirements. We start by choosing a shape for the graphane bilayer (GB) setup that allows for periodic replication of the confined structure, in this case the cell lengths in the periodic directions *x* and *y*. We then choose the composition of the linker as $(CH_2)_2$ and attach two tetramethylammonium (TMA) cations to one side of the GB. Next, we add a selected number of TIP3P water molecules [1], previously equilibrated in a classical MD bulk water simulation (using the TIP3P potential) [1], a carbonate molecule, and hydroxide ions between the graphane sheets by overlaying the bulk water simulation with the confined structure and selecting molecules with no spatial overlap with the cations. Finally, we set the distance between the two graphane layers, Δz, calculated as the distance between the hydrogen atoms on the inner surfaces. For systems **C1**, **C2**, **C3**, **C4**, and **3T3C** in which all water molecules fit in the spaces between the cations, Δz is set to the maximum possible height of the cations and is identical for all four systems (7.3 Å). [2,3] For system **C10**, which require additional room for the water molecules, the inter-sheet distance is

determined by fitting to the water molecules so as to achieve an effective maximum water density. [2]

After construction of the initial structures, *ab initio* molecular dynamics (AIMD) simulations [4,5] were run using the CPMD code. [6] We employed the dispersion-corrected atomic core pseudopotentials (DCACP) scheme[7] within the Kohn-Sham formulation of density functional theory (DFT) in order to ensure adequate treatment of the dispersion forces, and the B-LYP exchange-correlation functional [8,9], which has proven to be accurate in the treatment of the aqueous hydroxide ion.[10] A plane-wave (PW) basis set was employed to expand the Kohn-Sham orbitals with an energy cutoff of 80 Ry. The simulations were carried out using the mass of D instead of H for all hydrogen atoms in order to allow a larger time step to be employed and to reduce the importance of nuclear quantum effects.[11] The fictitious mass of the expansion coefficients was taken to be $\mu=600$ a.u., and a time step of 4 a.u. (0.096 fs) was employed for all simulations. Each system was equilibrated at the desired temperature using a massive Nosé-Hoover chain thermostat [12], followed by 15-20 ps of canonical (NVT) dynamics, also using a Nosé-Hoover chain thermostat, finally followed by ~80 ps of microcanonical (NVE) dynamics. The initial temperature for each NVE simulation is the final temperature obtained in the NVT simulation (which necessarily fluctuates around the target temperature). The temperature of the NVE simulation then oscillates around this initial temperature, as the temperature is not controlled under NVE. Due to deviations from the initial temperature set during the NVT run, the average temperature over the NVE trajectory is reported, rounded to the nearest five Kelvin.

For each atomic configuration generated in a simulation, the hydroxide ions in the system, whose oxygen atoms are designated as O*, were identified by finding the two oxygen atoms with only a single covalent hydrogen bond. Since each hydrogen can be uniquely assigned to a single oxygen based on the minimum O-H bond length, this assignment is unambiguous. All radial distribution functions were calculated using both the NVT and NVE trajectories, while all dynamic properties were obtained using only the NVE trajectories.

System Parameters for the Six Model AEMs

Table S1: System parameters for the six graphane bilayer structures presented in this study.

System Name	λ	Number of Cations	With / Without CO_2 / CO_3^{2-}	T (K)	Cation Spacing (Å)		Cell Geometry (Å)		
					Δx	Δy	x-axis	y-axis	z-axis
C1	1	2	W CO_2		10	6.6	10	13	7.3
C2	2	2	W CO_2	290	10	6.6	10	13	7.3
			WO CO_2	310					
C3	3	2	W CO_2	305	10	6.6	10	13	7.3
			WO CO_2	310					
C4	4	2	W CO_2	320	10	6.6	10	13	7.3
			WO CO_2	295					
C10	10	2	W CO_2	323	10	6.6	10	13	9.3
			WO CO_2	290					
3T3C	3	3	W CO_3^{2-}	280	10	6.6	10	19.6	7.3

Hydration Value (λ) :

The prevailing assumption is that certain regions in the AEM fuel cells will ultimately operate at low-hydration levels (regardless of the hydration value set at the beginning of operation) because of water consumption at the cathode as a result of the oxygen reduction reaction. Hence, it is crucial to characterize the hydroxide ion diffusion mechanisms at AEM under these conditions. For this purpose, we recently studied AEMs under low hydration values, at room temperature.[3]

In this work, we explore the effect of carbonation on hydroxide ions diffusion. As we find that the carbonation process is more pronounced at low hydration, we chose hydration values in the range of 1-4. To demonstrate the effect of the carbonation process at moderate hydration, we chose $\lambda = 10$. Based on our previous work comparing conditions at hydration values of $\lambda \geq 10$, we did not feel that additional higher hydration values would lead to qualitatively different results, which is why we chose $\lambda = 10$ as the maximum hydration state.

OO Radial Distribution Functions

Figure S1 presents the O_wO_w radial distribution functions (RDFs) and coordination numbers (CNs) values for the six systems. For all cases, the first peak, which represents the first solvation shell, corresponds roughly to that of bulk water (located at ~ 2.8 Å). However, as a result of the non-uniform water distribution, the CN values for the first and second solvation shells are lower than those in bulk solutions.[13,14] Specifically, we find the CN values of systems **C1**, **C2**, **C3**, **3T3C**, **C4**, and **C10**, for the first solvation shells to be approximately 0.5, 0.5, 1.4, 1.4, 1.8 and 3.2, respectively, and for the second solvation shell to be approximately 1, 1.6, 2.9, 2.9, 4.0 and 8.2, respectively. As was explained in our previous studies [13,14], for low hydration levels ($\sim\lambda < 8$), the non-uniform water distribution refers to the formation of spatially separated (by roughly 4 Å) water clusters in the vicinity of each ion. As a result, void areas are formed in the simulation cell. The specific patterns formed in these clusters influence the hydroxide and carbonate ions solvation structure and diffusion mechanisms as discussed in the main text, and in our previous studies. [2,3,15-18]
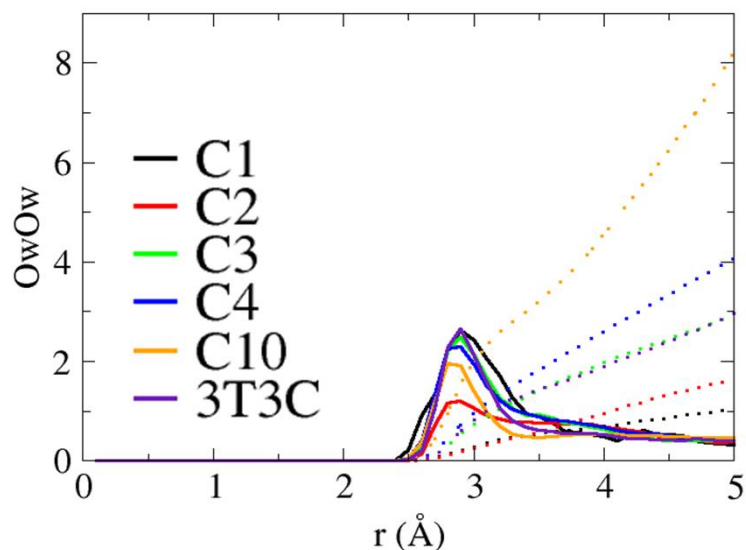
Figure S1: O_wO_w Radial distribution functions (RDFs) of the six systems. Black, red, green, blue, orange and purple curves represent systems **C1**, **C2**, **C3**, **C4**, **C10**, and **3T3C**, respectively. Colored dotted lines show the coordination numbers (CNs) for each system.

NO_w Radial Distribution Functions

Figure S2 presents the NO_w RDFs and CNs values for the six systems. For systems **C2**, **C3**, **C4**, and **C10**, we compare the results for previous systems studied without the presence of carbonate molecules (taken from Refs. [2,3,18]). For systems **C3**, **C4**, and **C10**, we find that adding CO_2 did not change the peak location nor the CN. Systems **C3** and **3T3C** have similar RDFs and CNs values. For systems **C1** and **C2**, the peak is located at 3.8 Å, while for system with $\lambda = 2$ in the absence of CO_2, the peak is shifted to 4.6 Å, however, the CNs are identical. To summary, we find that adding CO2 to the systems, has no dramatic effect on the NO_w RDFs and CNs.
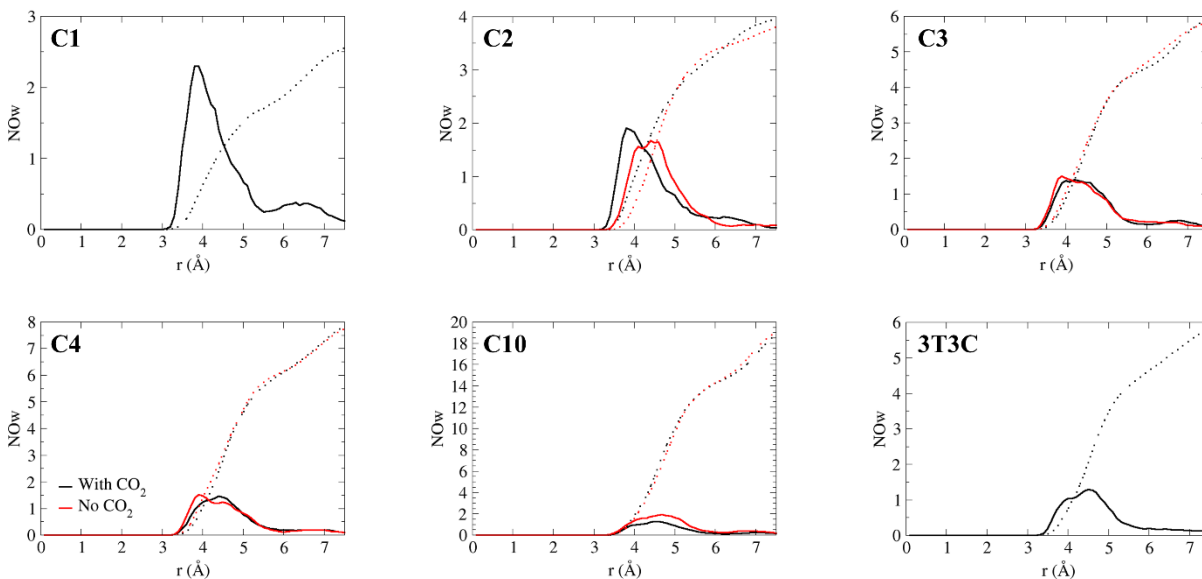
Figure S2: NO_w RDFs of systems **C1**, **C2**, **C3**, **C4**, **C10**, and **3T3C**, with and without carbonate molecules (black and red curves, respectively). Colored dotted lines show the CNs for each system.

NO[*] Radial Distribution Functions

Figure S3 presents the NO[*] RDFs and CNs values for systems **C2**, **C3**, **C4**, **C10** and **3T3C.** For systems **C2**, **C3**, **C4**, and **C10** we compare the results for previous systems studied without the presence of carbonate molecules (taken from Refs. [2,3,18]). For systems **C2** and **C3**, we find that in the presence of carbonate anion, the peak shifted further from the cations by approximately 1Å and 1.3Å, respectively. For systems **C2**, **C3** and **C4,** we find that in the presence of carbonate anion, the CN values decreased by approximately 0.7, 0.8 and 0.58 respectively. For system **C10**, we find that adding CO_2 to the system did no effect the peak location nor the CN values. For system **3T3C**, we find that the CN values are similar to the CN seen for systems **C3** and **C4**.
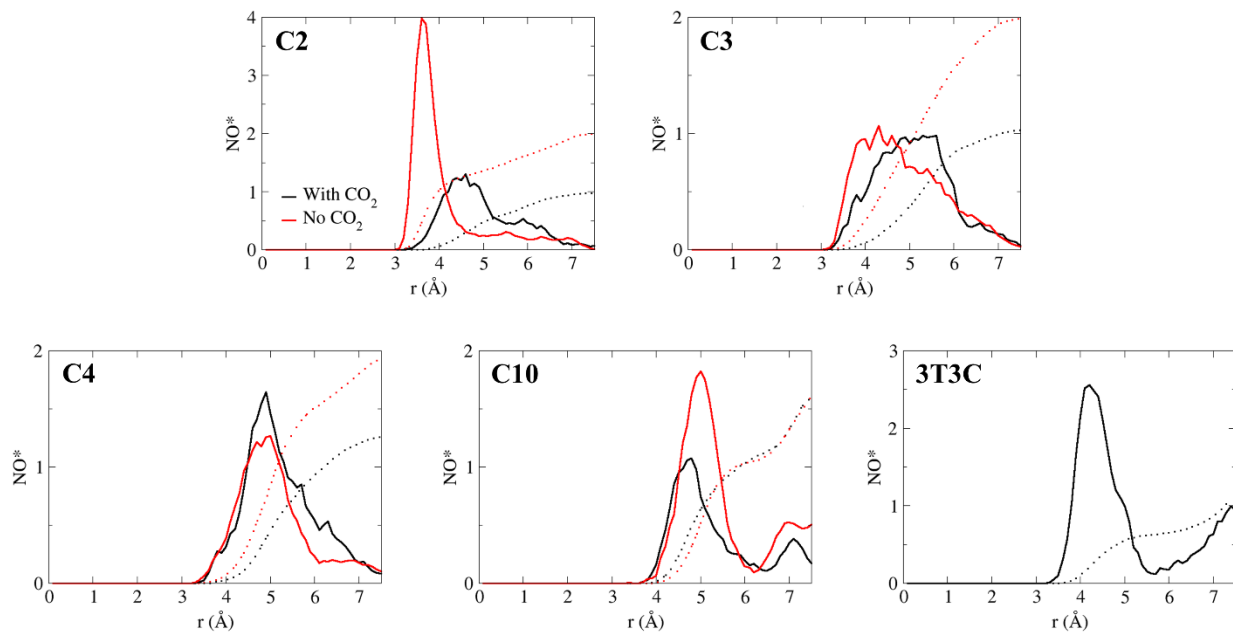
Figure S3: NO* RDFs of systems **C2**, **C3**, **C4**, **C10**, and **3T3C**, with and without carbonate molecules (black and red curves, respectively). Colored dotted lines show the CNs for each system.

Mean Square Displacements

The mean square displacement (MSD) is defined as:

$$MSD(t) = \frac{1}{N} \sum_{i=1}^{N} \left\langle \left| \mathbf{r}_i(0) - \mathbf{r}_i(t) \right|^2 \right\rangle$$

where $\mathbf{r}_i(t)$ is the position of molecule i at time t. In the long-time limit, the $MSD(t)$ becomes a linear function. According to the Einstein relation [19], in this limit, the diffusion coefficient is defined as the slope of the $MSD(t)$: $\lim_{t \to \infty} MSD = 2d * t * D$, where d is the dimensionality (in our calculations, $d = 1$ for the diagonal elements of the diffusion tensor and $d = 3$ for the total diffusion coefficient). To determine the MSD for OH^-, H_2O and carbonate anions with sufficient statistical sampling, we use a maximum dt of 8 ps, which is 10% of the trajectory length in this study. As these confined systems reach the linear regime after 2 ps, the diffusion coefficients are calculated using the slope of the $MSD(t)$ from 2 to 8 ps. However, since all of the species in all of the systems did not achieve a diffusion coefficient larger than 0.1 Å²/ps, we do not present the MSD plots. MSD plots for systems without carbon-containing species can be found in Refs. [2,3,18].

7

Diffusion Coefficients

Table S2: Diffusion constants obtained from the slope of the Mean Square Displacement in units of 10^{-8} m^2/s (i.e., Å^2/ps). *Results taken from: a) Ref. [20]; and b) Ref. [21] using the B-LYP functional.

System	With / Without CO_2 / CO_3^{2-}	T (K)	D_{OH^-} D	D_X	D_Y	D_Z	D_{H_2O} D	D_X	D_Y	D_Z
C1	W CO_2		---	---	---	---	0.10	0.11	0.16	0.03
C2	W CO_2	290	0.04	0.02	0.08	0.02	0.02	0.03	0.02	0.02
C2	WO CO_2	310	0.01	0.03	0.00	0.00	0.04	0.03	0.05	0.03
C3	W CO_2	305	0.03	0.00	0.03	0.00	0.05	0.05	0.09	0.01
C3	WO CO_2	310	0.15	0.19	0.27	0.01	0.09	0.08	0.16	0.02
C4	W CO_2	320	0.06	0.02	0.14	0.03	0.07	0.07	0.11	0.04
C4	WO CO_2	295	0.17	0.06	0.42	0.03	0.06	0.04	0.12	0.02
C10	W CO_2	323	0.06	0.06	0.12	0.00	0.04	0.05	0.06	0.01
C10	WO CO_2	290	0.12	0.02	0.33	0.00	0.01	0.02	0.01	0.00
T3C3	W CO_3^{2-}	280	0.02	0.01	0.05	0.00	0.03	0.03	0.04	0.01
*Bulk Solution	WO CO_2	298	0.45 [a]				0.17 [b]			

System	$D_{CO_2 \,/\, CO_3^{2-} \,/\, HCO_3^-}$			
	D	D_X	D_Y	D_Z
C1	0.00	0.00	0.00	0.00
C2	0.00	0.02	0.00	0.00
C3	0.00	0.01	0.00	0.00
C4	0.018	0.00	0.03	0.01
C10	0.00	0.00	0.01	0.00
T3C3	0.00	0.00	0.00	0.00

Table S3: O*O CN values for 1st and 2nd solvation shells

	Without Carbonate CN_1	With Carbonate CN_1	Without Carbonate CN_2	With Carbonate CN_2
C2	1.93	2.72	2.43	3.18
C3	2.74	3.36	3.84	5.12
C4	3.21	4.6	5.21	7.37
C10	4.05	4	11.24	10.5
3T3C	---	4.9	---	7.96

Hydroxide ions and Carbonate Anions Coordinates as A Function of Time

        To emphasis the non-diffusivity of the hydroxide ions and carbonate anions, we plot the coordinates of the hydroxide oxygens and the (tri)carbonate (i.e., CO_2 / HCO_3^- / CO_3^{2-}) carbons in each system as a function of time along the *x*-, *y*- and *z*- axes separately in Figures S4 and S5, respectively.
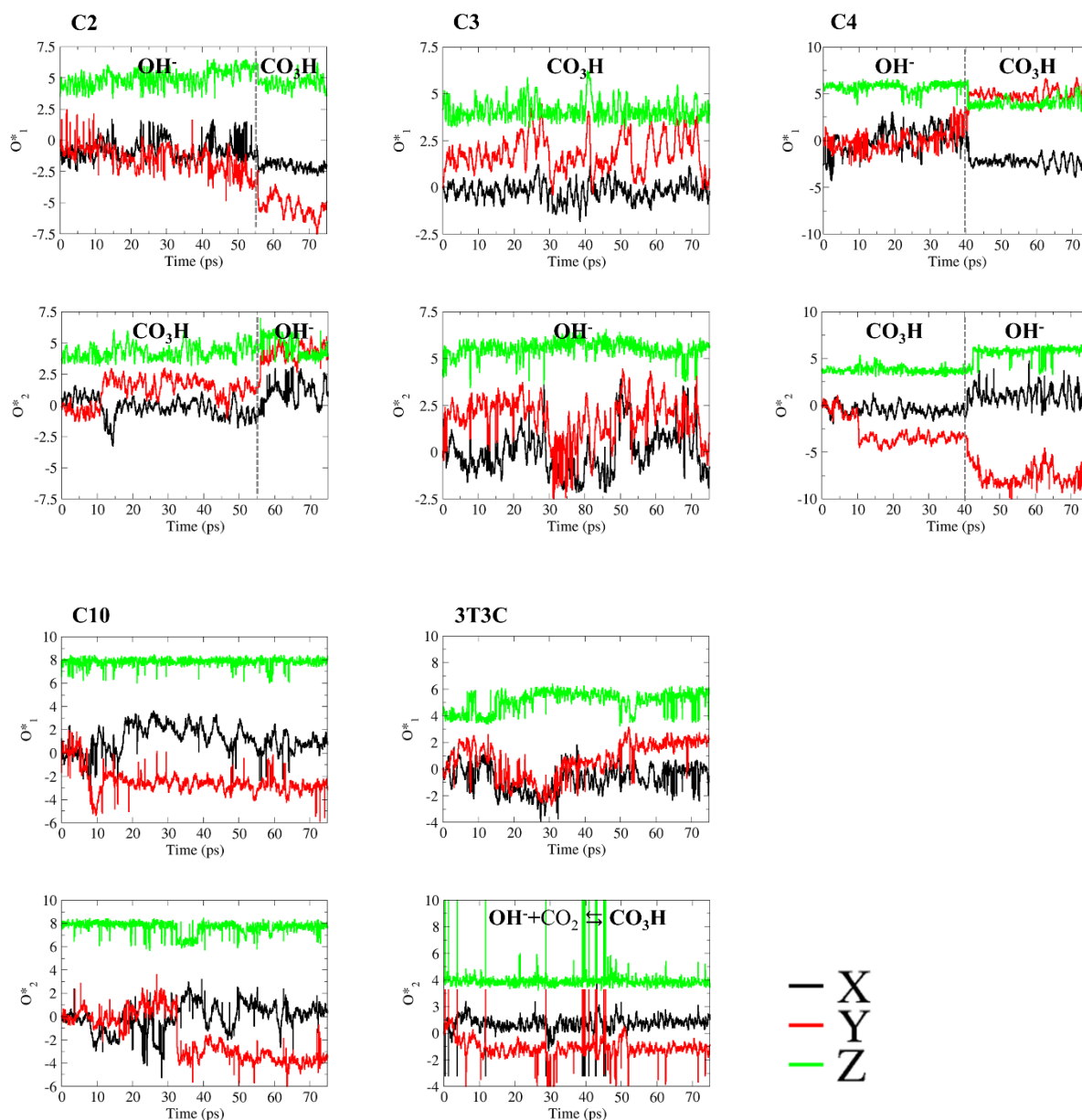

Figure S4: Hydroxide ion oxygen coordinates as a function of time (black, red and green curves for *x, y* and *z*- coordinates, respectively) for O^*_1 and for O^*_2 during the NVE simulations for systems **C2**, **C3**, **C4**, **C10** and **3T3C**.
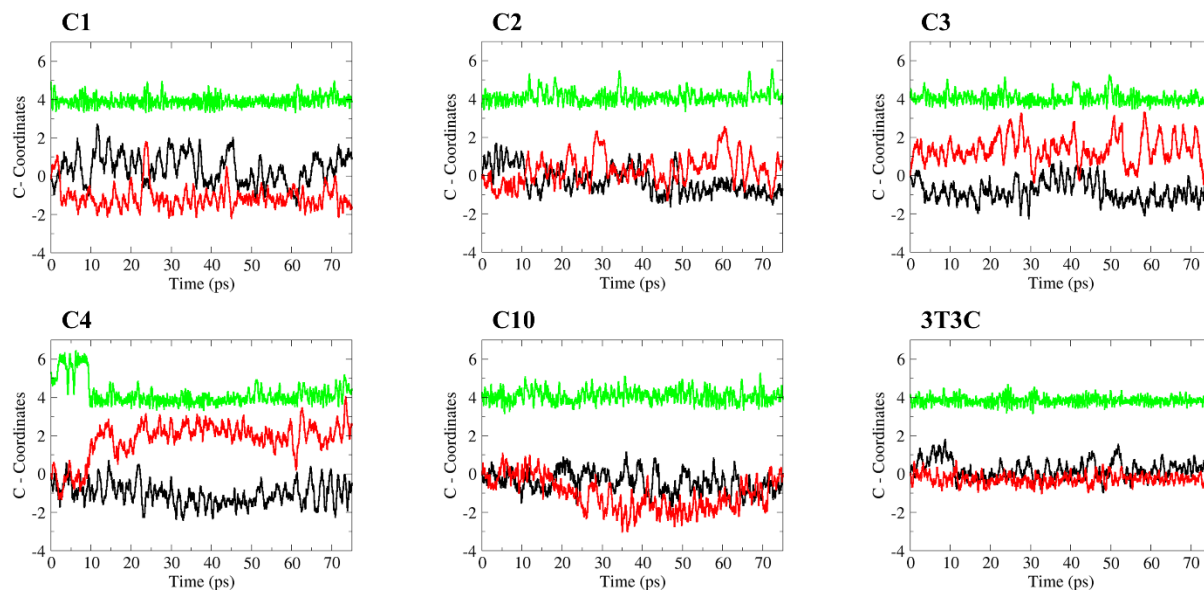
10

Figure S5: (Tri)carbonate carbon coordinates as a function of time (black, red green curves for x, y and z coordinates, respectively) during the NVE trajectory, for the six systems.

Table S4:

The time (in ps) required for the forward path of the 1st reaction to occur ($OH^- + CO_2 \rightarrow HCO_3^-$) for systems **C1**, **C2**, **C3**, and **C4**, at different initial conditions. The results for the 1st initial conditions are taken from the main text Figure 4.

	1st initial structure	2nd initial structure	3rd initial structure	4th initial structure
C1	0.0377	0.081	---	---
C2	0.0957	0.200	0.078	0.090
C3	3.92	4.2	7.11	6.54
C4	29.417	0.25	>100ps	---

11

Experimental Details

Preparation of the PSU-based AEMs

AEMs based on Polysulfone (PSU), were synthetized as described in details in our recent work. [22] In brief, PSU has been functionalized with trimethylamine (TMA) by two steps-procedure, in order to get TMA-PSU polymer, in chlorine form (Cl⁻ form) used to prepare self-standing membranes via solution casting method (see Figure S6). The membrane in Cl⁻ form is then soaked in a proper solution for 48 h, to get the ion-exchange reaction: in a 1 M KOH aqueous solution to get the OH⁻ form, in a 1 M $KHCO_3$ aqueous solution to get the HCO_3^- form, and in a mixture $KOH/KHCO_3$ 1:1 mixture, to get the mixed (OH^-/HCO_3^-) form. After the 48 h of soaking, the membranes were rinsed in deionized water to remove alkaline excesses.

In order to get the ^{13}C-NMR measurements, the $KHCO_3$ aqueous solution was prepared starting from the KOH solution in which $^{13}CO_2$ gas was bubbled so that all OH⁻ ions reacted to give $H^{13}CO_3^-$. Similarly, the mixture solution was obtained by mixing in equal amounts a 1M KOH solution with a 1M $H^{13}CO_3^-$ solution.
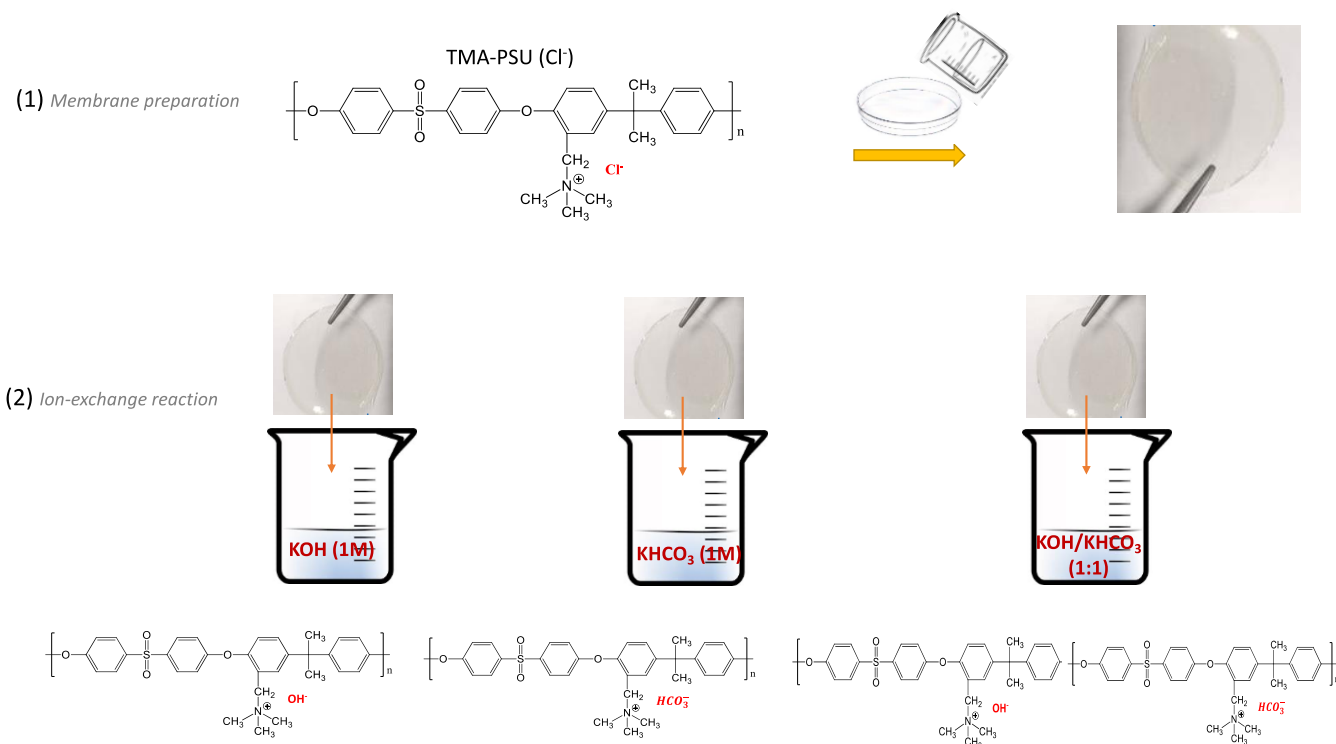

Figure S6: Scheme of the (1) AEM preparation and (2) subsequent ion-exchange procedure.

Water uptake (WU%) was measured by soaking the dried membrane (w_{dry}) in deionised water at room temperature for 24 hours. It was then quickly dried with tissue paper to remove surface water droplets and weighted (w_{wet}). The water uptake was calculated by Eq. 1, and reported as an average of at least three independent measurements, while λ was calculated by Eq. 2. The average IEC of TMA-PSU based AEM is 0.81 meq/g.

$$wu\% = \frac{W_{wet} - W_{dry}}{W_{dry}} \cdot 100; \ [\%] \tag{1}$$

$$\lambda = \frac{wu}{MM_{H_2O}} \times IEC \tag{2}$$

NMR investigation: ^{1}H and ^{13}C PFG experiments

The membrane (in OH^{-}, H^{13}CO$_3^{-}$ and OH^{-}/ H^{13}CO$_3^{-}$ mixture forms) swollen in water was wiped off surface drops with blotting paper and allowed to equilibrate under a flow of N$_2$ until it reached a weight and thus the desired λ value, at which time it is inserted into an NMR tube and sealed.

NMR measurements were performed on a Bruker AVANCE 300 wide bore spectrometer working at 300 MHz on ^{1}H and 75 MHz on ^{13}C. The employed probe was a Diff30 Z-diffusion 30 G/cm/A multinuclear with substitutable RF inserts. The self-diffusion coefficients (D) have been measured by Pulsed Field Gradient Stimulated-Echo (PFG-STE) sequence [23] consisting of three 90° RF pulses (π/2-τ_1- π/2- τ_m- π/2) with two gradient pulses applied after the first and the third RF pulses. At time $\tau = 2\tau_1 + \tau_m$ the echo is found. The FT echo decays were analyzed by means of the relevant Stejskal–Tanner equation:

$$I = I_0 e^{-\beta D} \tag{3}$$

with I and I_0 representing the intensity/area of a selected resonance peak with and without gradients, respectively, D the self-diffusion coefficient and β the field gradient parameter. This latter is defined by Eq. 4:

$$\beta = [(\gamma g \delta)^2 (\Delta - \frac{\delta}{3})] \tag{4}$$

where g, δ and Δ are the amplitude, duration, and time delay of the gradient field, respectively. The parameters chosen for ^{1}H-PFG PFG measurements were: diffusion time (Δ) of 10 ms, pulse

length (δ) of 1 ms, gradient amplitude varying from 100 to 900 G/cm and the number of scans was 8. The parameters chosen for ^{13}C-PFG measurements were: diffusion time (Δ) between 15 and 25 ms, pulse length (δ) between 1 and 3 ms, gradient amplitude varying from 100 to 900 G/cm. Due to the very low standard deviation of the fitting curve and repeatability of the measurements, the uncertainties in D values were lower than 3%. Measurements were conducted by increasing temperature step by step from 20 °C to 80 °C, every 10 °C, leaving the sample to equilibrate at each temperature for about 15 min.

References

[1]   P. Mark and L. Nilsson, "Structure and Dynamics of the TIP3P, SPC, and SPC/E Water Models at 298 K," *J. Phys. Chem. A*, 105, 9954–9960, 2001.

[2]   T. Zelovich, Z. Long, M. Hickner, S. J. Paddison, C. Bae, and M. E. Tuckerman, "Ab initio Molecular Dynamics Study of Hydroxide Diffusion Mechanisms in Nano-Confined Structural mimics of Anion Exchange Membranes," *J. Phys. Chem. C*, 123, 4638–4653, 2019.

[3]   T. Zelovich, L. Vogt-Maranto, M. A. Hickner, S. J. Paddison, C. Bae, D. R. Dekel, and M. E. Tuckerman, "Hydroxide Ion Diffusion in Anion Exchange Membranes at Low Hydration: Insights from Ab *initio* Molecular Dynamics," *Chem. Mater*, 31, 5778–5787, 2019.

[4]   M. E. Tuckerman, "Ab Initio Molecular Dynamics: Basic Concepts, Current Trends and Novel Applications," *J. Phys. Condens. Matter*, 14, R1297–R1355, 2002.

[5]   D. Marx and J. Hutter, *Ab Initio Molecular Dynamics: Theory and Implementation, in Modern Methods and Algorithms of Quantum Chemistry*, Vol.1. Juelich: Forschungszentrum, 2000.

[6]   D. M. J. Hutter, A. Alavi, T. Deutsch, M. Bernasconi, S. Goedecker and M. T. and M. Parrinello, "CPMD, IBM Corporation 1990–2009 and MPI für Festkörperforschung 1997–2001; see www.cpmd.org, 2009." .

[7]   I.-C. Lin, M. D. Coutinho-Neto, C. Felsenheimer, O. A. von Lilienfeld, I. Tavernelli, and U. Rothlisberger, "Library of Dispersion-Corrected Atom-Centered Potentials for

Generalized Gradient Approximation Functionals: Elements H, C, N, O, He, Ne, Ar, and Kr," *Phys. Rev. B*, 75, 205131–205135, 2007.

[8] A. D. Becke, "Density-Functional Exchange-Energy Approximation With Correct Asymptotic Behavior," *Phys. Rev. A*, 38, 3098–3100, 1988.

[9] C. Lee, W. Yang, and R. G. Parr, "Development of the Colle-Salvetti Correlation-Energy Formula into A Functional of the Electron Density," *Phys. Rev. B*, 37, 785–789, 1988.

[10] M. E. Tuckerman, A. Chandra, and D. Marx, "Structure and Dynamics of OH$^-$ (aq)," *Acc. Chem. Res.*, 39,. 151–158, 2006.

[11] D. Marx and J. Hutter, *Ab Initio Molecular Dynamics: Basic Theory and Advanced Methods*, Cambridge. Cambridge: Cambridge University Press, 2009.

[12] G. J. Martyna and M. L. Klein, "Nose-Hoover Chains: The Canonical Ensemble via Continuous Dynamics," *J. Chem. Phys.*, 97, 2635–2643, 1992.

[13] M. E. Tuckerman, K. Laasonen, M. Sprik, and M. Parrinello, "*Ab Initio* Molecular Dynamics Simulation of the Solvation and Transport of Hydronium and Hydroxide Ions in Water," *J. Chem. Phys.*, 103, 150-161, 1995.

[14] M. Tuckerman, K. Laasonen, M. Sprik, and M. Parrinello, "Ab Initio Molecular Dynamics Simulation of the Solvation and Transport of H_3O^+ and OH$^-$ Ions in Water," *J. Phys. Chem*, 99, 5749–5752, 1995.

[15] T. Zelovich and M. E. Tuckerman, "Water Layering Affects Hydroxide Diffusion in Functionalized Nanoconfined Environments," *J. Phys. Chem. Lett*, 11, 5087–5091, 2020.

[16] T. Zelovich, K. I. Winey, and M. E. Tuckerman, "Hydronium Ion Diffusion in Model Proton Exchange Membranes at Low Hydration: Insights from Ab Initio Molecular Dynamics," *J. Mat. Chem. A*, 9, 2448–2458, 2021.

[17] T. Zelovich and M. E. Tuckerman, "OH$^-$ and H_3O^+ Diffusion in Model AEMs and PEMs at Low Hydration: Insights from Ab Initio Molecular Dynamics," *Membranes (Basel).*, 11, 355–368, 2021.

[18] T. Zelovich, L. Vogt-Maranto, C. Simari, I. Nicotera, M. Hickner, S. J. Paddison, C. Bae,

D. R. Dekel and M. E. Tuckerman, "Non-Monotonic Temperature Dependence of Hydroxide Diffusion in Anion Exchange Membranes," *Chem. Mater.* 23, 2133−2145, 2022.

[19] M. E. Tuckerman, *Statistical Mechanics : Theory and Molecular Simulation.* Oxford University Press, 2010.

[20] Z. Ma and M. E. Tuckerman, "On the Connection Between Proton Transport , Structural Diffusion , and Reorientation of the Hydrated Hydroxide Ion as a Function of Temperature," *Chem. Phys. Lett*, 511, 177–182, 2011.

[21] H. S. Lee and M. E. Tuckerman, "Dynamical Properties of Liquid Water From Ab Initio Molecular Dynamics Performed in the Complete Basis Set Limit," *J. Chem. Phys.*, 126, 164501–164516, 2007.

[22] C. Simari, E. Lurfrano, M. H. U. Rehman, A. Zhegur-Khais, S. Haj-Bsoul, D. R. Dekel, and I. Nocitera, "Effect of LDH Platelets on the Transport Properties and Carbonation of Anion Exchange Membrane," *Electrochim. Acta, 403,* 139713-139723, 2021.

[23] J. E. Tanner, "Use of the Stimulated Echo in NMR Diffusion Studies," *J. Chem. Phys.*, 52, 2523–2526, 1970.